Integrated strategy of network analysis prediction and experimental validation to elucidate the possible mechanism of compound Turkish gall ointment in treating eczema

Xuan Ma (mx646@163.com)
Xinjiang Medical University
Meng Hao
Xin jiang Qi Mu Medical research institue
Ming Hui Zhang
Xin Jiang Qi Mu Medical research Institute
Ya Zeng
Xin Jiang Qi Mu Medical Research Institute
Qing Qing Yang
Xin Jiang Qi Mu Medical Research Institute
Lu Zhao
Xin Jiang Qi Mu Medical Rearch Institute
Chen Yang Fan
Xinjiang Qimu Medical Research Institute
Zhi Hong Ji
Xin Jiang Key Laboratory of Generic Technology of Traditional Medicine(Ethnic Medicine) Pharmacy of
Ke Ao Li
Xin Jiang Qi Mu Medical Research Institute
Zhi Jian Li
Xinjiang Uygur Medical Research Institute
Maimaiti Mirzat
Xin Jiang Qi Mu Medical Research Institute
Jihong Nie
Xin Jiang Key Laboratory of Processing and Research of Traditional Medicine

Research Article

Keywords: Eczema, TLR4/NF-κB signaling pathway, CTGO, HPLC fingerprint, network analysis

Posted Date: April 14th, 2022

DOI: https://doi.org/10.21203/rs.3.rs-1516290/v1

Abstract

Background: Compound Turkish gall ointment (CTGO) has been widely used as a folk medicine for a long history in Xinjiang for the treatment of eczema. CTGO is currently in the pre-investigational new drug application stage, but its pharmacologic

-al mechanisms of action have not yet been clarified.

Methods: First, a sensitive and reliable ultra-high performance liquid chromatograph

-y-Q exactive hybrid quadrupole-orbitrap high-resolution accurate mass spectrometry (UHPLC-Q-Orbitrap HRMS) technique was established. Second, an integrative strategy of network analysis and molecular docking based on identified and retrieved ingredients was implemented to investigate the potential targets and pathways involved in the treatment of eczema with CTGO. Ultimately, Sprague-Dawley (SD) rats with eczema were prepared to verify the predicted results. The skin conditions of the rats were observed, evaluated, and scored. Skin tissues were observed by hematoxylin-eosin (HE) staining, while serum interferon-γ (IFN-γ) and interleukin-4 (IL-4) levels were determined by enzyme-linked immunosorbent assay (ELISA). The expression levels of toll-like receptor 4 (TLR4), nuclear factor kappa-B p65 (NF-κB p65), interleukin-1β (IL-1β), and tumor necrosis factor-α (TNF-α) were detected by real-time quantitative polymerase chain reaction (RT-qPCR).

Results: A total of 29 compounds were preliminarily identified. We found 38 active components and 58 targets for the treatment of eczema; these involved 118 signaling pathways related to inflammation, immunity, and apoptosis. CTGO significantly improved the skin surface and histopathological characteristics of eczema-affected rats, downregulated the expression of IL-4, TLR4, NF-κB (p65), IL-1β, and TNF-α, and upregulated the expression level of IFN-γ.

Conclusion: We predicted, and validated our prediction, that CTGO may be used to treat eczema by affecting the TLR4/NF-κB signaling pathway, which provides guidance for future experimental studies.

Background

Eczema is a chronic inflammatory skin disease with exudative tendency. Its main clinical manifestations are erythema, blisters, erosion, and pruritus [1]. Modern medicine believes that the main etiology of eczema is T cell-mediated immune damage. Antihistamines and glucocorticoid drugs are often used for clinical treatment of eczema; however, these drugs often lead to adverse reactions and frequent recurrence, and also have a high cost [2–3]. Traditional Chinese medicine (TCM) has a long history in the treatment of eczema. Three pathogenic factors of rheumatic fever are considered the main causes of eczema. Treatment mainly focuses on removing wind and dampness, cooling blood, and detoxification [4–6]. Network analysis is based on a “drug–composition–target–disease” relationship characterised by comprehensive analysis, and has been introduced to evaluate the constituents and action mechanism of TCM in view of its systematic and holistic coincidences [7–9]. CTGO comprises Turkish galls and comfrey.Turkish gall is a traditional Uygur medicine distributed in the Mediterranean coast, Arabia, Turkey, Greece, and Iran. It is the gall of Quercus infectoria Oliv. The main components of CTGO are tannin and gallic acid, which have anti-inflammatory, drying, astringent, and hemostatic effects [10–11].Comfrey is the dried root of Arnebia euchroma(Royle) Johnst,distributed in Xinjiang, Tibet, Gansu, and other places, with numerous naphthoquinones and polysaccharides, and it has anti-bacterial, anti-inflammatory, and immunological regulatory effects [12]. Comfrey has the effects of dryness and dampness astringency, clearing heat and cooling blood, detoxification.In long-term clinical application, CTGO has been shown to have a good effect on eczema..Based on the network analysis of the potential components, targets, and mechanisms of CTGO in the treatment of eczema, as well as verification by animal experiments, we explored the therapeutic effect and mechanism of CTGO in a rat model of eczema to provide a theoretical basis for the treatment of eczema with CTGO.

We systematically expounded the possible targets and related pathways of CTGO in treating eczema by integrating UHPLC-Q-Orbitrap HRMS, network analysis, molecular docking analysis, and experimental evaluation using molecular biology. Figure 1 shows the flow chart of this whole analysis.

Materials And Methods

Materials andequipment

Low (0.035 g/g,batchNo.20200506), medium (0.07 g/g, batchNo.200401), and high (0.14 g/g, batchNo.20200507) concentrations of CTGO (NEW CICON Pharmaceutical Co., Ltd), Gallic acid (China Institute for Food and Drug Control, content: 91.5%, Batch No. 110831-201906), Gallic acid methyl ester (Chengdu Pufei De Biotech Co., Ltd., content: 98.0%, Batch No. 17092604), Ethyl gallate (Chengdu Pufei De Biotech Co., Ltd., content: 98.0%, Batch No. 19042902), Ellagic acid (China Institute for Food and Drug Control, content: 88.8%, Batch No. 111959-201903), β,β-Dimethylacrylalkannin (China Institute for Food and Drug Control, content: 98.0%, Batch No. 111689-201805), L-shikonin (China Institute for the Control of Pharmaceutical and Biological Products, Batch No. 110769-200506), Methanol and acetonitrile of HPLC grade were purchased from Sigma-Aldrich Company. All other reagents were of analytical grade and supplied by Tianjin Beilian Fine Chemicals Development Co., Ltd. Compound dexamethasone acetate cream (China Resources Sanjiu Medical and Pharmaceutical Co., Ltd., 20201024X), 2, 4-dinitrochlorobenzene (DNCB) (Shanghai Jiudin Chemical Technology Co., Ltd., 97-00-7), IL-4, INF-γ test box (Shanghai Enzyme Linked Biotechnology Co., Ltd., 05/2020, 06/2020), PCR kit (Beijing Quanshijin, AQ601-01), Microscope (Leica, Germany, EQ2016-037), Thermo Fisher, Multiskan FC, and an electronic balance (Germany Sartorius, CPA124S) were obtained.

Experimental animals

SixtySprague-Dawley (SD) rats (180–220 g body weight and aged 5–7 weeks) were purchased from the Laboratory Animal Center ofXinjiang Medical University(License number:SCXK (new) 2018-0002).Allof therats were fed in an environment free of specific pathogens: temperature 20–26°C, humidity 40%–70%, artificial light, 12-h light-dark cycle, and free access to water and food.

Database and analysis software

The following databases were used: TCMSP (http://tcmspw.com/index.php/), CNKI (https://www.cnki.net/),CTD(http://ctdbase.org/),ETCM(http://www.tcmip.cn/ETCM/index.php/Home/Index/),TCMID(http://47.100.169.139:8000/tcmid/),BATTCM (http://bionet.ncpsb.org.cn/batman-tcm/), GEO (https://www.ncbi.nlm.nih.gov/geo/), DrugBank (https://go.drugbank.com/), STRING (https://string-db.org/),PubChem (https://pubchem.ncbi.nlm.nih.gov/), and PDB (http://www1.rcsb.org/). The softwareCytoscape 3.7.2,R3.6.1 language, Chem3D, PyMOL, AutoDock Vina-1.5.6,and BIOVIA Discovery Studio 2020 were used.

Untargeted UHPLC-Q-Orbitrap MS analysis

Chromatographic separation was performed on aQ-Exactive-Plus (Thermo Fisher Scientific Inc., Waltham, MA, USA)using aKromasil Classic 100-5-C18 column (100 ×4.6 mmi.d., 5 μm) at30°C with a flow rate of 1.0mL/min and awavelength of 300 nm.The mobile phase consisted of water containing 0.1% formic acid (solvent system A) and acetonitrile (solvent system B), andgradient elutionwas conductedas follows: 0–5 min,5% B, 5–45 min, 5%–12% B, 45–50 min, 12% B, 50–80 min, 12–20% B, 80–95 min, 20%–25% B, 95–105 min,25%–67% B, 105–115 min, 67%–70% B, 115–125 min,70%–75% B, 125–135 min, 75% B. Ten microlitresof the sample solution was injected for analysis.

Mass detection was performed using an UHPLC-Q-Orbitrap HRMS equipped with a

Dual ESI source operating in both the positive and negative modes with the following operating parameters: ESI spray voltage, –2.8 kV (positive ion, 3.2 kV), sheath gas, 40 arb, auxiliary gas, 10 arb, air curtain gas (CUR), 35, ion source temperature (heat temp), 350°C, capillary temperature, 300°C, –70 V, focusing voltage (FP), –350 V, and DP2, –10 V. The data dependent acquisition(DDA)mode was adopted for sample analysis: the collection range of q-orbitrap was 100–1500 m/z, and the fragment ion scanning range was 50–1500 m/z. Collision gas (NCE): 20, 40, 60. The mass spectrometry (MS) resolution was 70,000 full width at half maximum (FWHM) (200 m/z), and the MS^2 resolution was 17600 FWHM (200 m/z). The Xcalibur 4.0 software package was used for data acquisition and analysis (Thermo Fisher Scientific Inc., Waltham, MA, USA).

To prepare the sample, we first weighed 0.05 gofTurkish galls beforeplacingintoa conical flask. Next, 25 mL of 80% methanol was added before a 1-h reflux in a water bath at 75°C. Then,a pipette was used to transfer 1 mL of the supernatant into a 5-mL volumetric flask. In parallel, 0.1 g of Comfrey was weighed precisely and placed into another conical flask, before adding 50 mLof chloroform and subjecting it toa 1-h reflux in a water bath at 75°C. Next, the sample was filtered, and the solvent was evaporatedinthewater bath. Theresidue was transferred intothe abovementioned 5-mLvolumetric flask with about 4 mL acetonitriletobring the total volume to 5 mL.

Network Analysis

“Turkish galls”and“comfrey”weresearched for inthe TCMSP, CTD, TCMID, ETCM, and BATMAN-TCMdatabases andtheliterature to obtain the components of Turkish galls and comfrey. These agentswere combined with the compounds identified by UHPLC-Q-Orbitrap-HRMS to buildthe active ingredient databaseof CTGO.Targetscorresponding to the componentswere obtainedthrough the TCMSP and BATMAN-TCM databases, and a target database of CTGO was constructed. “Eczema” was searched inGEO and DrugBank databasesto obtain eczema targets. R3.6.1 language software was used to obtain the intersection targets of drugs and diseases.

The intersection targets and corresponding componentsand the top 20 pathways of significance were inputto Cytoscape 3.7.2 software to construct a “component-target-pathway” network, and the size of degree value was reflected by the size of the nodes.All intersection targets were imported into the String data platformto builda protein-protein interaction(PPI)network. The PPI networkwasimportedthe Cytoscape 3.7.2 softwareto build with PPI topology analysis. Gene Ontology (GO) and Kyoto Encyclopedia of Genes and Genomes (KEGG) enrichment analyses were performed on the intersection targetsbyR3.6.1 language software, and a threshold $q< 0.05$ was set. Biological processes and target pathways with significant differences were screened.

Molecular docking

The three core components of gallic acid, ellagic acid, and shikonin in the component-target network were docked with the four core targets of TNF, IL-1β, TLR4, and albumin (Alb) in the PPI network. First, the composition and target files were downloaded from PubChem and PDB, respectively.The componentfile’s energy minimization was completed by Chem3D, and the targetfile’s dewatering and impurity removal were completed by PyMOL.Next, the file was converted to PDBQT format using AutoDock Vina. The active pocket of the target was determined, molecular docking was performed, and binding energy values were obtained.The best docking model diagram was drawn by BIOVIA Discovery Studio.Finally, the binding ability was evaluated by the affinity of the component and the target.An affinity < 0 means that the ligand and the receptor can bind spontaneously, and the lower the affinity, the stronger thebinding effect. An affinity < –5.0 kcal/mol indicatesgood bindingactivity.

Animal experiment

Sixty rats were randomly divided into a normal group, a model group, a positive group (compound dexamethasone acetate cream), a CTGO high-dose group, a CTGO medium-dose group, and a CTGO low-dose group, with 10 rats in each group. Except for the normal group, the rats in the other groups were treated with 7% DNCB solution by rubbing the solution on the back to establish the eczema model. The hair on the neck (A: 2 cm × 2 cm) and back (B: 4 cm × 4 cm) of the animals was removed using an electric shaver. The rats were sensitized by applying 100 μL of 7% DNCB acetone solution with a pipetting gun on the skin of site A. Severe pruritus, frequent scratching, and rolling behaviors were observed in rats, lasting for about 2 h. After 1 week, 200 μL of 7% DNCB acetone solution was applied to site B for excitation. Theratswere stimulated once every 5 days, and severe pruritus could be seen in rats, with frequent scratching and rolling behavior in each stimulation. Erythema, papules, edema, scratches, and desquamation gradually appeared on the skin at site B. After each stimulation,

the skin lesions were recorded and scored. After six sessions of stimulation, erythema, papules, scab, and exudation appeared in skin lesions on the back of each rat, at which point the stimulation was stopped, indicating that the model had been successfully established(Miao MS, et al., 2017).

Eachgroup was administered low (0.035 g/g), medium (0.07 g/g), or high (0.14 g/g) concentrations of CTGO, and the positive group was administered compound dexamethasone acetate cream (0.75 mg/g, 0.3 g each time, once a day). The normal and model groups were administered with saline.After smearing the experimental drug,2–3 layers ofmedical gauze were wrapped and fixed with a non-irritating adhesive tape. After 4 h, the covering was removed and washed with warm pure water for continuous administration for 14 days.

After the last administration, the rats were fasted with water for 12 h. The rats were mildly anesthetized with 1% sodium pentobarbital (4 mL/kg, i.p.). Blood samples were collected from the abdominal aorta, whichwere placed in a centrifuge tube for 30 minand centrifuged at 3000 rpm for 10 min at 4°C. The supernatant was stored at –20°C. One part of the obtained skin tissue was immersed in 10% neutral formalin for fixation, and the other part was stored at −80°C.

On the 1st, 5th, 10th, 15th, 20th, 25th, 30th, and 35th days of modeling, and on the 0th, 9th, and 14th days of administration, the grades of erythema, edema, exudation, desquamation, liche-like change, desquamation, and other indexes were evaluatedfrom 1 to 4 grade. After 14 days of administration, Skin conditionwerephotographed, andnaked eye observation was performed.

Skin tissuewasremoved from10% neutral formalinsolution, dehydrated,permeated, paraffin impregnated, embedded, sectioned, stained, and sealed. Histomorphological observation was performed with a microscope, and radiographs were taken.

The levels of IFN-γ and IL-4 in the serum of rats were determined according to the instructions of the ELISA kit.

The mRNA expression levels of TLR4, NF-κB (p65), IL-1β, and TNF-α in skin tissue samples were detected by RT-qPCR. RNA was extracted, its purity was determined, and cDNA was obtained by reverse transcription. PCR upstream and downstream primers were added (2 μL each, refer (Table 1)for specific information) to the PCR reaction system of 20 μL according to the kit instructions. The reaction procedures were as follows: pre-denaturation at 95°C for 5 min, denaturation at 95°C for 5s, and annealing at 60°C for 35s, detection was conducted after 45cycles. The $2^{-\triangle\triangle CT}$ method was used to analyze the difference in target gene expression between the control group and test groups.

Table 1. PCR primer sequence

Gene	Sequence
β-actin	F-CCCATCTATGAGGGTTACGC
	R-TTTAATGTCACGCACGATTTC
TLR4	F-TCCTTTCCTGCCTGAGACCA
	R-TGTCTCAATTTCACACCTGGAT
NF-κB	F-TGTATTTCACGGGACCTGGC
	R-CAGGCTAGGGTCAGCGTATG
IL-1β	F-AAATGCCTCGTGCTGTCTGA
	R-TTGGGATCCACACTCTCCAG
TNF-α	F-GTCCCAACAAGGAGGAGAAGTT
	R-CTCCGCTTGGTGGTTTGCTA

Statistical analysis

All data are presented as the mean±standard deviation. All statistical analyses were conducted using SPSS software, version 23.0.the data of multiple groups of measurement data were analyzed by ANOVA, and multiple comparisons were analyzed by LSD.p< 0.05 was considered statistically signifcant.

Results

Results of UHPLC-Q-Orbitrap-HRMS

The samples were collected by UHPLC-Q-Orbitrap-HRMS using positive and negative ion simultaneous scanning mode,and 29compounds were preliminarily identified, as shown in (Fig.2) and (Table 2).

Table 2 Analysis results of UHPLC-Q-Orbitrap-HRMS

No.	tR (min)	$[M-H]^-$	$[M+H]^+$	Error (ppm)	Formula	MS/MS	Identification
1	2.48	191.05595		4.9171	C7H12O6	173 (5), 127 (10), 93 (20), 85 (40)	Quinic acid
2	2.79	331.06683		2.5990	C13H16O10	271 (10), 211 (50), 169 (100), 125 (60)	Galloyl-glucoside
3	3.20	331.06680		2.5068	C13H16O10	271 (20), 211 (30), 169 (100), 125 (60)	Galloyl-glucoside
4	3.36	481.06274		3.0404	C20H18O14	331(10), 313 (5), 301 (100), 275 (60),	HHDP-glucoside
5	4.87	169.01407		4.9285	C6H12O7	257 (30), 169 (40), 125 (30)	Gallic acid
6	7.44	483.07849		3.2285	C20H20O14	125 (100)	Di-galloyl-glucoside
7	10.90	483.07962		3.2285	C20H20O14	313 (20), 271 (5), 211 (5), 169 (100), 125 (70)	Di-galloyl-glucoside
8	23.98	483.07837		2.9785	C20H20O14	313 (20), 271 (5), 211 (5), 169 (100), 125 (70)	Di-galloyl-glucoside
9	24.94	183.02925		2.4656	C8H8O5	331 (10), 313 (20), 271 (30), 211 (80), 169 (100), 25 (70)	Methylgallate
10	25.42	483.07858		3.4181	C20H20O14	169 (20), 125 (30)	Di-galloyl-glucoside
11	26.93	635.08850		0.9618	C27H24O18	331 (10), 313 (20), 271 (70), 211 (70), 169 (100), 125 (60)	Tri-galloyl-glucoside
12	29.54	635.08960		2.6917	C27H24O18	483 (20), 465 (60), 313 (30), 169 (100), 125 (70)	Tri-galloyl-glucoside
13	32.91	635.0899		3.8451	C27H24O18	483 (20), 465 (40), 313 (32), 169 (100), 125 (80)	Tri-galloyl-glucoside
14	35.79	635.09015		3.9612	C27H24O18	483 (20), 465 (80), 313 (30), 169 (100), 125 (80)	Tri-galloyl-glucoside
15	37.56	197.04541		4.8734	C9H10O5	169 (50), 125 (40)	Ethyl gallate
16	42.42	300.99780		–0.3017	C14H6O8	257 (10), 229 (10), 185 (5)	Ellagic acid
17	66.51	165.05573		6.6912	C9H10O3	137 (80), 108 (20), 93 (80	Methyl p-hydroxybenzoate
18	80.22	287.09277		4.7837	C16H16O5	218 (100), 190 (20), 173 (5)	L-shikonin
19	84.29	627.2245		3.3077	C36H36O10	567 (80), 507 (100), 463 (50), 410 (20), 347 (10), 284 (10)	6-(11'-Deoxyalkannin)-alkannin /shikonin isobutyrylate
20	97.44	387.14536		3.9409	C21H24O7	285 (5), 269 (70), 251 (60), 225 (30), 186 (20), 117 (100)	β-Hydroxy isovaleryl Shikonin
21	100.55	329.10321		3.7852	C18H18O6	269 (100), 251 (90), 225 (40), 186 (50)	Acetylshikonin
22	101.65		271.0963	–0.5217	C16H16O4	253 (60), 243 (20), 229 (90), 225 (40), 137 (70), 93 (20)	Shikonin
23	101.69	429.15564		2.9022	C23H26O8	369 (5), 269 (100), 251 (40), 225 (30), 186 (20)	β-Acetoxy isoamyl acarnin
24	106.18	357.13461		3.7750	C20H22O6	269 (100), 251 (70), 225 (60), 186 (30)	Isobutyryl Shikonin
25	110.49		271.0963	–0.5217	C16H14O4	253 (60), 229 (100), 165 (20), 137 (80)	Deoxyshikonin
26	110.51	369.13449		3.3216	C21H22O6	269 (100), 251 (80), 225 (50), 186 (40)	β,β'-Dimethyl acryloyl Shikonin
27	111.596	455.35361		3.5914	C30H48O3	153 (5), 113 (10), 69 (30)	Ursolic acid
28	112.85	269.08228	271.09647	–0.0715	C16H14O4	253 (60), 229 (100), 165 (30), 137 (70)	Deoxyshikonin-isomer
29	112.90	371.15012		3.2361	C21H24O6	269 (100), 251 (70), 225 (30), 186 (40)	α-Methyl n-butyryl shikonin/ isovaleryl Shikonin

Network pharmacological analysis

Sixty-nine active components of CTGO were obtained, of which 10 were obtained from Turkish galls and 59 were obtained from comfrey, corresponding to a total of 886 targets. A total of 193 eczema-related targets were obtained. Fifty-eight targets of CTGO and eczema intersection were finally obtained.

After matching 58 intersection targets with 69 active ingredients, 38 active ingredients with a therapeutic effect on eczema were finally obtained, as shown in (Table 3). A total of 38 active ingredients and 58 intersection targets and the top 20 pathways of significance were imported into Cytoscape3.7.2software to construct the “component-target-pathway” regulation network of TCM prescriptions. The top four core components in the ranking of degree value

were gallic acid, palmitic acid, ellagic acid, and shikonin. The top 10 degree value core targets were RELA, TNF, IL1B, TGFB1, TGFB2, TLR4, IFNG, TGFBR2, TGFBR1, STAT3, as shown in (Fig.3).

Table 3 "Component-target" active ingredient

Traditional Chinese medicine	MolId	MolName	Number of eczema-related targets
Turkish galls	MOL000513	Gallic acid	21
Turkish galls	MOL000069	Palmitic acid	20
Turkish galls	MOL001002	Ellagic acid	17
Turkish galls	MOL002037	Amentoflavone	4
Turkish galls	MOL001907	Progallin A	3
Turkish galls	MOL000359	Sitosterol	3
Turkish galls	MOL001906	Methylgallate	2
Turkish galls	MOL000569	Digallate	1
Comfrey	MOL000069	Palmitic acid	20
Comfrey	MOL000223	Caffeic acid	9
Comfrey	MOL007731	Arnebinol	9
Comfrey	C016101	Shikonin	9
Comfrey	MOL007720	(2R)-3-oxo-2-phenylbutanenitrile	8
Comfrey	MOL000511	Ursolic acid	7
Comfrey	MOL000131	Eic	6
Comfrey	MOL000675	Oleic acid	5
Comfrey	MOL007722	Isoarnebin 4	5
Comfrey	MOL007719	Arnebin 7	4
Comfrey	MOL000359	Sitosterol	3
Comfrey	MOL003616	Isobutyryl shikonin	3
Comfrey	MOL007714	1-methoxyacetylshikonin	3
Comfrey	MOL007723	Alkannan	3
Comfrey	MOL007740	[(1R)-1-(5,8-dihydroxy-1,4-dioxo-2-naphthyl)-4-methyl-pent-3-enyl] 2-methylpropanoate	3
Comfrey	MOL001494	Mandenol	2
Comfrey	MOL002691	Iva	2
Comfrey	MOL003619	[(1R)-1-(5,8-dihydroxy-1,4-dioxo-2-naphthyl)-4-methyl-pent-3-enyl] 3-methylbutanoate	2
Comfrey	MOL007715	[(1R)-1-(5,8-dihydroxy-1,4-dioxo-2-naphthyl)-4-methyl-pent-3-enyl] propanoate	2
Comfrey	MOL007716	Acetylshikonin	2
Comfrey	MOL007717	Alkannin beta,beta-dimethylacrylate	2
Comfrey	MOL007732	Arnebinone	2
Comfrey	MOL007737	Alpha-methyl-n-butylshikonin	2
Comfrey	MOL007724	Senecic acid	1
Comfrey	MOL007727	Ethyl senecioate	1
Comfrey	MOL007728	Lithospermidin A	1
Comfrey	MOL007729	Shikonofuran C	1
Comfrey	MOL007730	Shikonofuran B	1
Comfrey	MOL007734	5-[(E)-5-(3-furyl)-2-methyl-pent-2-enyl]-2,3-dimethoxy-p-benzoquinone	1
Comfrey	MOL007736	Lithospermidin B	1
Comfrey	MOL007738	Beta-acetoxyisovalerylshikonin	1
Comfrey	MOL007739	[(1R)-1-(5,8-dihydroxy-1,4-dioxo-2-naphthyl)-4-methyl-pent-3-enyl] 3-hydroxy-3-methyl-butanoate	1

The network consisted of 58 nodes and 390 edges. The average node degree value was 13.4, and the PPI enrichment *P*-value was<1.0×10^{-16}.The top four targets in degree value included Alb, tumor necrosis factor (TNF), IL1β, and TLR4.In PPI topology analysis, the six topological eigenvalues of "closeness centrality (CC)," "betweenness centrality (BC)," "eigenvector centrality (EC)," "local average connectivity (LAC)," "degree centrality (DC)," and "network centrality (NC)" were used as filter conditions. Targets whose topological eigenvalues were all greater than their corresponding medians were used as core targets, and two rounds of analysis were performed. Fifteen core targets were obtained in the first round and four in the second round, as shown in (Fig.4).

In this study, GO and KEGG enrichment analyses and visualization processing were performed on 58 intersections of CTGO and eczema using the Bioconductor bioinformatics software package. The GO functional annotation results showed that a total of 1420 ($p < 0.05$) GO functional enrichment items were obtained, including 1316 biological processes (BPs),75 molecular functions (MFs), and 29 cellular components (CCs), as shown in (Fig.5). KEGG pathway enrichment analysis results showed that a total of 118 ($p < 0.05$) signaling pathways were obtained, as shown in (Fig.6).

The molecular docking affinity of gallic acid, ellagic acid, shikonin, and TNF, IL-1β, TLR4, and Alb was < 0, demonstrating that the core components and core targets can bind spontaneously and form a relatively stable structure (Table 4). The molecular docking structure is shown in (Fig 7).

Table 4 Results of molecular docking between core components and targets

Traditional Chinese medicine	MolId	MolName	Target	PDB	Affinity (kcal/mol)	Center			Size		
						x	y	z	x	y	z
Turkish galls	MOL000513	Gallic acid	TNF	6RMJ	−6.8	−1.641	65.631	127.508	40	40	40
			IL1β	5I1B	−5.2	11.308	13.79	2.447	62	40	40
			TLR4	2Z66	−6.8	−25.107	−20.278	27.945	46	60	126
			Alb	1AO6	−6.1	28.423	8.392	23.263	40	46	46
Turkish galls	MOL001002	Ellagic acid	TNF	6RMJ	−9.1	−1.641	65.631	127.508	40	40	40
			IL1β	5I1B	−7.0	11.308	13.79	2.447	62	40	40
			TLR4	2Z66	−8.7	−25.107	−20.278	27.945	46	60	126
			Alb	1AO6	−8.5	28.423	8.392	23.263	40	46	46
Comfrey	C016101	Shikonin	TNF	6RMJ	−7.8	−1.641	65.631	127.508	40	40	40
			IL1β	5I1B	−7.1	11.308	13.79	2.447	62	40	40
			TLR4	2Z66	−8.9	−25.107	−20.278	27.945	46	60	126
			Alb	1AO6	−8.5	28.423	8.392	23.263	40	46	46

Animal experiment

After 14 days of administration, the back skin of rats in the normal group was pale red, delicate, and tender, with a soft texture. The back skin lesions of the rats in the model group were obvious, with skin erythema, infiltration, scales, scabs, rough and thickening texture, pigmentation, and scratches, which still met the diagnostic criteria for chronic eczema. Compared to the model group, the erythema, infiltration, scales, and scabs on the back of rats in each administration group were significantly reduced or subsided. Compared to the normal group, the apparent score of rats in the model group was significantly increased ($p < 0.01$). Compared to the model group, the apparent scores in each administration group were significantly decreased ($p < 0.01$), as shown in (Table 5.)

Table 5 Apparent score of zone B (excitation zone) in each group

Grouping	Score
Normal group	0
Model group	$5.4 \pm 0.8^{\#\#}$
Positive (0.75 mg/g) group	3.4 ± 0.8**
CTGO low-dose (0.035 g/g) group	2.8 ± 0.4**
CTGO medium-dose (0.07 g/g) group	2.5 ± 1.4**
CTGO high-dose (0.14 g/g) group	2.0 ± 0.7**

Compared to the normal group $^{\#}p < 0.05$, $^{\#\#}p < 0.01$, compared to the model control group $^{*}p < 0.05$, $^{**}p < 0.01$

The thickness of the cuticle, epidermis, and dermis in the normal group was normal. Model group rats showed chronic eczema, including hyperkeratosis, parakeratosis, hypertrophy of the granular layer, hypertrophy of the spinous layer, and infiltration of numerous inflammatory cells in the epidermis/dermis.

After 14 days of administration, hyperkeratosis, parakeratosis, hypertrophy of the granular layer, and hypertrophy of the spinous layer were inhibited in each administration group, and the infiltration of inflammatory cells in the epidermis/dermis was reduced. The results are shown in (Fig.8).

Compared to the normal group, the levels of IFN-γ and IL-4 in the model group were significantly decreased ($^{\#}p < 0.05$). Compared to the model group, the level of IFN-γ in the administration groups was significantly increased ($^{**}p < 0.01$) and that of IL-4 was significantly decreased ($^{*}p < 0.05$, **P p <0.01) (Fig.9).

Compared to the normal group, the contents of TLR4, NF-κB, IL-1β, and TNFα in the skin tissue of rats in the model group were significantly increased ($^{\#\#}p <$ 0.01, $^{\#\#\#}p < 0.001$, or $^{\#\#\#\#}p < 0.0001$). Compared to the model group, the contents of IL-1β and TNFα in the skin tissue of rats in the positive group and CTGO low-, medium-, and high-dose groups were significantly decreased ($^{*}p < 0.05$, $^{**}p < 0.01$, and $^{***}p < 0.001$, respectively), and the contents of TLR4 and NF-κB in the skin tissue of rats in the CTGO low-, medium-, and high-dose groups were significantly decreased ($^{**}p < 0.01$, $^{***}p < 0.001$, and $^{****}p < 0.0001$, respectively). Compared to the positive group, the contents of TLR4 and NF-κB in the skin tissue of rats in the medium- and high-dose CTGO groups were significantly decreased ($^{\square}p < 0.05$ and $^{\square\square}p < 0.01$, respectively) (Fig.10).

Discussion

TCM compounds have multi-component and multi-target synergistic effects, and it has been widely used in clinical practice because of its clear curative effect and minor side effects. CTGO has shown good clinical efficacy in the treatment of eczema, but its mechanism of action remains unclear. Based on network pharmacological analysis, this study investigated the pharmacodynamics and action mechanism of CTGO in a rat model of eczema.

In this study, a combined strategy of phytochemistry, network analysis, molecular docking, and basic experiment was used to assess the active constituents and potential molecular mechanisms of CTGO on eczema. First, the chemical composition of CTGO was characterized by UHPLC-Q-Orbitrap HRMS for the first time. A total of 28 constituents, mainly belonging to polyphenols, naphthalene quinones, and anthraquinones, were identified, and 69 components were further reviewed from databases and previously published papers. Next, 38 key components were further filtered through network analysis.

The component-target-pathway network contained 38 active ingredients. The common active components of gallic galls and comfrey are palmitic acid and β-sitosterol. Their common targets are the core targets of TNF and IL-1β, which rank highly in degree value. The top two components in degree value were gallic acid and ellagic acid, which are the main components of gallic galls, and have 11 common targets, namely, TNF, TGFβ1, RELA, PTGS1, PTGS2, NOS2, MMP9, IL-1β, CYP1B1, CYP1A1, and Alb. All of the targets are closely related to inflammatory, immune, and metabolic reactions. Shikonin is the main chemical component of comfrey; it can act on nine eczema-related targets, among which TNF and PTGS2 are the common targets of shikonin, gallic acid, and ellagic acid. Gallic acid has a good antibacterial effect, and it can effectively inhibit Staphylococcus aureus, Pseudomonas aeruginosa, Candida albicans, and E. coli [13]. Gallic acid is also a powerful anti-inflammatory agent that inhibits the secretion of pro-inflammatory cytokines, TNF, IL-6, and IL-1, and it indirectly inhibits lipopolysaccharides (LPSs) in the cell wall of Gram-negative bacteria to induce an inflammatory response [14–15]. Ellagic acid is a polyphenolic dilactone, which is a dimer derivative of gallic acid, and it has a variety of biological effects, including antioxidant, anti-inflammatory, anti-proliferative, and antiviral effects [16]. Studies have shown that ellagic acid can reduce leukocyte infiltration and inhibit cell recruitment and the expression of cytokines (IL-4, IL-5, and IL-13) in a time- and dose-dependent manner [17]. Shikonin is the main chemical component of comfrey, which has anti-inflammatory, anti-tumor, bacteriostatic, liver protection, and immune regulatory effects [18]. Studies have shown that shikonin may inhibit the expression of SP, NK-1R, and ICAM-1 in the skin tissue of eczema model mice, inhibit mast cell degranulation, and alleviate the symptoms of eczema inflammatory injury [19].

The PPI network contains 58 core targets for the treatment of eczema, reflecting the multi-target characteristics of CTGO in the treatment of eczema. TNF-α, IL1β, and IL-4 are important cytokines in the process of skin immunity and inflammation. Under the action of allergens in the skin system, numerous inflammation-mediated factors, such as TNF-α, IL1β, and IL-4, are secreted during epidermal keratinization, all of which interact with each other in the pathogenesis of eczema, thus influencing the development and prognosis of the disease [20–21]. TLR4 is an important pattern recognition receptor that promotes the expression of TNF-α and IL1β by activating NF-κB [22]. TLR4 896A > G loci polymorphism is closely associated with disease severity in patients with eczema [23].

The 38 active ingredients act on 58 targets related to eczema; all of these 58 targets are connected with 118 pathways closely related to inflammation and immunity. All of the above components, targets, and pathways form a network, which may be the mechanism by which CTGO functions to treat eczema. The toll-like and NF-κB pathways are among the first 30 pathways significantly associated with CTGO in the treatment of eczema and are closely related to inflammatory responses. The toll-like pathway affects the NF-κB pathway through regulating NF-κB, and the NF-κB pathway then regulates the downstream of the toll-like pathway. As NF-κB connects the two pathways, they are closely related and mutually regulated. Moreover, core targets with high degree values are key upstream and downstream targets involved in the two pathways, such as TLR4, TNF-α, and IL1β in the PPI network. Therefore, this study speculates that the toll-like and NF-κB signaling pathways may be the main way by which CTGO functions in the treatment of eczema. Thus, the TLR4/NF-κB signaling pathway was selected for validation, and its downstream indicators were selected as the core targets in the PPI network such as TNF-α and IL1β. Toll receptors are a class of highly conserved pattern recognition receptors. TLR4 recognizes various ligands of microorganisms and undergoes dimerization upon ligation. MyD88 and non-MyD88 pathways activate mitogen-bound protein kinase, activate NF-κB, upregulate inflammatory cytokines and chemokines, and induce inflammation. It plays an important role in the pathogenesis of eczema [24–25].NF-κB is a nucleoprotein factor that exists widely in eukaryotic cells, and its pathological activation is involved in the occurrence and development of various inflammatory diseases, including eczema and asthma. When cells are exposed to external stimulation, the complex of NF-κB and its inhibitory protein IκB are activated, and IκB is phosphorylated, ubiquitinated, and degraded. The resulting free NF-κB is transferred to the nucleus, and the target genes are activated. Inflammatory factors, such as IL-1β and TNF-α, are highly expressed, which can induce the expression of various genes and regulate the inflammatory response. It is involved in the occurrence and development of related diseases like eczema and asthma [26–28].

In this study, the rat eczema model was induced by DNCB. When the body is re-exposed to the same antigen after being stimulated by DNCB through the skin, a type IV allergic reaction characterized by skin damage occurs. Repeated stimulation can produce clinical manifestations similar to eczema, and the coincidence degree with the main symptoms of eczema in Chinese medicine is > 70%. Following establishment of the model, many indicators can be used to judge whether the model has been established successfully and whether the drug has a therapeutic effect after administration. Among them, the apparent indexes belong to the core indexes, such as the skin lesion area, itching condition, fur gloss, and skin erythema and edema. Pathological indexes are directly related indexes, and local histopathological changes of skin are reliable indexes to evaluate the degree of skin lesions. Biochemical indexes are indirectly related indexes, and IL-4 and other biochemical indexes will increase after the animal eczema model has been successfully established [29]. After CTGO treatment, the eczema apparent index in the skin area of the lesion was significantly reduced, histopathological manifestations were significantly improved, and the expression level of IL-4 in serum was significantly reduced, indicating that CTGO had a good therapeutic effect on the eczema in rats.

Patients with eczema have a severe inflammatory response, and many inflammatory factors play a key role in the occurrence and development of eczema. The TLR4/NF-κB signaling pathway is involved in the inflammatory response, where TLR4 recognizes endogenous ligands and is activated via identifying related ligands, and the signal conduction through the MyD88 pathway leads to the activation of NF-κB. This signaling ultimately results in the production of a large amount of IL-1β, TNF-α, and other inflammatory factors, which promote cell proliferation and repair. However, with the excessive activation of NF-κB, these inflammatory factors will also be excessively released; then, the responsive activation of TLR4 forms a vicious cycle, which leads to uncontrollable inflammatory response. Consequently, the epidermis produces excessive inflammatory reactions, and the tissue organs are damaged, which result in the occurrence and development of eczema. The results of the animal experiments indicated that CTGO could significantly reduce the expression of IL-1β, TNFα, TLR4, and NF-κB. These changes in key genes suggest that the mechanism of CTGO in treating eczema may be related to the effect of the TLR4/NF-κB signaling pathway [30–31].

Conclusions

In conclusion, CTGO may influence the TLR4/NF-κB signaling pathway by acting on TNF-α, IL-1β, IL-4, and other core targets closely related to eczema through the action of gallic acid, ellagic acid, and shikonin, thereby improving the pathological manifestations and inflammatory response of eczema-affected rats and playing a role in the treatment of eczema. Future in-depth validation studies will be performed to better understand the specific mechanism of the action of CTGO in the treatment of eczema.

Abbreviations

CTGO,Compound Turkish gall ointment, UHPLC-Q-Orbitrap HRMS,ultra-high performance liquid chromatography-Q exactive hybrid quadrupole-orbitrap high-resolution accurate massspectrometry, SD,Sprague-Dawley, HE,hematoxylin-eosin, IFN-γ,interferon-γ , IL-4,interleukin-4, TLR4,toll-like receptor 4, NF-κB p65,nuclear factor kappa-B p65, IL-1β,interleukin-1β, TNF-α,tumor necrosis factor-α, RT-qPCR,real-time qu-antitative polymerase chain reaction, TCM,Traditional Chinese medicine, SD,Sprague-Dawley, DNCB,2, 4-dinitrochlorobenzene, PPI,protein-proteininteraction, GO,Gene Ontology, KEGG,Kyoto Encyclopedia of Genes and Genomes, Alb,albumin.

Declarations

Acknowledgements

Not applicable

Author contributions

N-JH and M-X conceived and designed the experiment, H-M and F-CY conducted an analysis of the network pharmacology of gallic ointment in the treatment of eczema, Z-MH and Z-Y conducted an Fingerprint analysis, M-X, Y-QQ, Z-L, J-ZH, L-KA, Li-ZJ carried out the experiments, M conducted the data sorting and statistical analysis, M-X and N-JH wrote the manuscript.All authors contributed to preparation and editing of this manuscriptthe for intellectual content.

Funding

This work was supported by Key R&D project of Xinjiang Uygur Autonomous Region[grant numbers 2018B03018-2]

Availability of data and materials

The datasets used and analyzed during the current study are available from the corresponding author on reasonable request.

Ethics approval and consent to participate

The animal experiments were approved by the Institutional Animal Care and Use Committee, Research Institute of Xinjiang Uygur medicine (nGLP-2020002).

Consent for publication

Not applicable.

Competing interests

The authors declare that they have no competing interests.

Author details

[1]College of Pharmacy, Xinjiang Medical University, Urumqi 830011, Xinjiang, China.[2]Xinjiang Qimu Medical Research Institute, Urumqi 830002, Xinjiang, China.[3]Xinjiang Key Laboratory of Generic Technology of Traditional Chinese Medicine (Ethnic Medicine) Pharmacy, Urumqi 830002, Xinjiang, China.[4]Xinjiang Uygur Medical Research Institute, Urumqi 830011, Xinjiang, China.[5]Department of Pharmacy, Affiliated Hospital of Traditional Chinese Medicine, Xinjiang Medical University, Urumqi 830011, Xinjiang, China.[6]Xinjiang Key Laboratory of Processing and Research of Traditional Chinese Medicine，Urumqi 830011, Xinjiang, China.

References

1. Boyle R.J,Shamji M.H.Aetiology and prevention of eczema.Clinical and experimental allergy.2021:51(3):380-381.
2. Caglayan Gall.Causes and Symptoms of Atopic Eczema.Journal of Allergy and Therapy.2021, 12(3),1-1.
3. Chen X,Huang L.X,Li X.H,Wu Q.Y,Tian J.Data Mining Research on the Law of External Treatment of Eczema with Traditional Chinese Medicine.Liaoning Journal of Traditional Chinese Medicine.2021, 48(09):86-90.
4. Gong J.Study on the pharmacokinetics of gallic substances and its main active components.Guangzhou University of Chinese Medicine.2018.
5. He W.Z,Du HNew progress in the prevention and treatment of eczema by traditional Chinese and western medicine.Gansu Medicine.2018, 37(08):693-696.
6. Hui Y,Li J.T,Wei H.L,Yan S.G.Notch and TLR4/NF-κB signaling pathways in the treatment of ulcerative colitis with 6-gingerenol.Chinese Journal of Pharmacy.2020, 55(16):1331-1338.
7. Jia G.Q,Shen G.Q,Zhang Q,Zhu M.J.Toll receptor mediated expression of MYD88/TRAF6/NF-κB.Journal of Emerging InfectiousDiseases.2017, 2(02):104-107+111.
8. Jiang Y,Wang C.H,Li L,Dan C.X,Jiang H.H.Study on the regulation mechanism of acupoint combination and combination based on TLR4/NF-kB pathway on stresgastric ulcer.Shi Zhen Traditional Chinese Medicine and Materia Medica.2020, 31(5):1264-1267.
9. Li Z.Y.Effect of Jinque Liangxue Jiedu Granules on Immune Regulation of Rat Eczema Model.Heilongjiang University of Traditional Chinese Medicine.2018.
10. Li Z.J,Lan X.Y,Han R.l,Wang J,Huang Y.Z,Sun J.J,Guo W.J,Chen H.miR-2478 inhibits TGFβ1 expression by targeting the transcriptional activation region Downstream of the TGFβ1 promoter in Dairy Goats.Scientific reports2017, 7:42627.
11. Lin H.Y,Wang X,He C,Zhou Z.L,Yang M.K,Wen Z.L,Han H.W,Lu G.H,Qi J.L,Y-ang Y.H.Progress on biosynthesis and function of the natural products of Zi Cao as a traditional Chinese medicinal herb.Yi chuan Hereditas2021, 43(5):459-472.
12. Long F.Studies on the isolation and identification of the chemical constituents of gallic fruit.Shihezi University.2017.
13. Miao M.S.Specifications for the preparation of animal models of eczema (draft).Chinese Journal of Experimental Formulas.2017, 23(24):6-10.
14. Qian X,Li H.T,Zeng W.X,Shi X.F.Research progress on chemical constituents pharmacological action and product application of Persia sinensis.China Wild Plant Resources 2021, 40(3):52-56+69.
15. Rogerio Alexandre.P,Fontanari Caroline,Borducchi Erica,Keller Alexandre.C,Russo Momtchilo,Soares Edson.G,Albuquerque Deijanira.A,Faccioli Lúcia.H. Anti-inflammatory effects of Lafoensia pacari and ellagic acid in a murine model of asthma.European journal of pharmacology.2008, 580(1-2):262-270.
16. Shi H.Y,Xi Y.L.Research Progress on the Biological Activity of Gallic Acid. Journal of Jilin Medical College.2020, 41(02):146-149.
17. Stephan Weidinger,Natalija Novak,Norman Klopp,Hansjörg Baurecht,Stefan Wagenpfeil,Lars Rummler,Johannes Ring,Heidrun Behrendt,Thomas Illig.Lack of association between Toll-like receptor 2 and Toll-like receptor 4 polymorphisms and atopic eczema.The Journal of allergy and clinical immunology.2006, 118(1):277-279.
18. Tang J.L,Zhou L,Sun Z.Y,Zhang L.C.Application of network analysis in the treatment of autoimmune diseases with traditional Chinese medicine.Chinese Pharmacology Bulletin.202l, 37(3):323-327.
19. Wang C.H,Wang X,Shen Y.W,Liu K.Study on the therapeutic effect and mechanism of shionin on eczema in mice.China Pharmacist.2021, 24(3):456-461.
20. Wang Z.S,Lin Y,Ma S.F,Ding W.L.Diagnosis and treatment of eczema from Yin and Yang in traditional Chinese medicine.China Clinician Journal.2020, 48(1):125-126.
21. Qu S.H.Mangiferin inhibits mastitis induced by LPS via suppressing NF-κB and NLRP3 signaling pathways.International immunopharmacology.2017, 43:85-90.
22. Wang X.H,Zhao H.Q,Ma C.H,Lv L,Feng J.P,Han S.G.Gallic acid attenuates al- lergic airway inflammation via suppressed interleukin-33 and group 2 innate lymphoid cells in ovalbumin-induced asthma in mice.International Forum of Allergy & Rhinology2018, 8(11):1284-1290.
23. Wang Y.G,Dou Y.Q,Feng J,Xu C.Y,Wang Q.Efficacy of Liangxue Guyuan decoction on radiation-induced intestinal injury in rats via the toll-like receptor 4/myeloid differentiation primary response 88/nuclear factor-kappa B pathway. Journal of Traditional Chinese Medicine2021, 41(02):254-261.
24. Wu N,Huang Y.X,Shi X,Chen J.L,Peng L.F,Yang L.L,Xu H,Sun J.F,Liu H.Effects of Gannudu smoke on TLR4-MyD88-NF-κB signaling pathway in rats with chronic bronchitis.Journal of Guizhou Medical University.2020, 45(11):1283-1288.
25. Wu XL,Zhong C,Shi J.M.Biological effects of ellagic acid.China Forestry By-products.2019, (01):73-78.
26. Yan D.D,Huang F.Research progress on pathogenesis of eczema.Modern Health Care.2017, (4):44.
27. Yin Y,Gu W,Lu Y.Effects of Qingying Decoction on the Expression of TNF-α and IL-4 in Acute Eczema in Rats.Shanghai Journal of Traditional Chinese Medicine.2019, 53(07):70-74.

28. Yuan T,Cui L.L,Wang Y,Li Y,Liu Y.The latest development of Chinese medicine network analysis.Journal of Traditional Chinese Medicine.2021, 49(01):101-106.
29. Zhang X.C,Chen P,Kong Q.R,Wang L,Wang Y.H,Shen Z.Q,Chen P.Expression of CD4, CD8, IL-4 and TNF-α in eczema guinea pigs.Shi Zhen Traditional Chinese Medicine and Traditional Chinese Medicine.2020, 31(4):789-792.
30. Zhang X,Yanan W,Chong X,WeiZ.K,WangJ.J,YangZ.T,FuY.H.Resveratrol inhibits LPS-induced mice mastitis through attenuating the MAPK and NF-κB signaling pathway.Microbial pathogenesis.2017, 107:462-467.
31. Zhuang Y.S,Zhang R,Xv Y.L.Application progress of network analysis in Chinese medicine research.Journal of Nanjing University of Traditional Chinese Medicine.202l, 37(1):156-160.

Figures

Figure 1

shows the flow chart of this whole analysis

Figure 2

UHPLC-Q-Orbitrap-HRMS total ion flow atlas.Representative base peak chromatogram of CTGO in the positive and negative ions mode, respectively.

Figure 3

CTGO-eczema-pathway “component-target” network.Compound-target–pathway network (Blue rectangles represents target, Circles represents common compound. Yellow squares represents pathway. It’s a positive proportional relationship that between the node size and the degree).

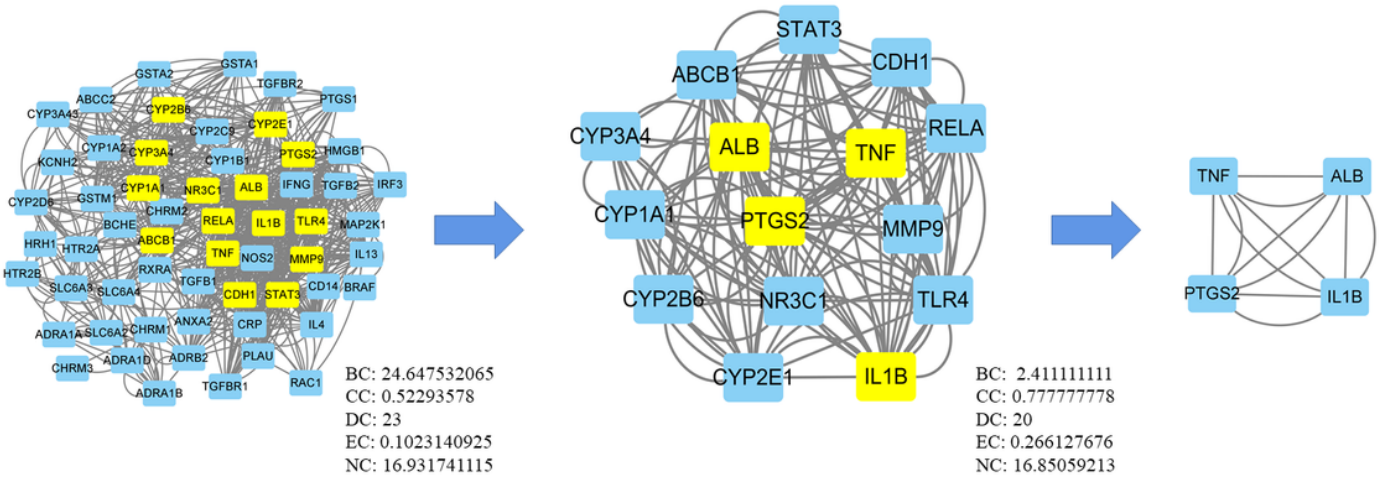

Figure 4

PPI topology analysis.Targets are indicated by rectangles.The nodes representing candidate compounds are shown as yellow rectangles.

Figure 5

CTGO-eczema GO analysis

Figure 6

CTGO-eczema KEGG analysis.Top 30 KEGG pathway enrichment candidate targets for CTGO activity against eczema for each expression profile. Pathways with significant changes($p < 0.05$) were identified.The vertical coordinates represent the KEGG pathway with significant enrichment, and the horizontal

coordinates represent the number of differentially expressed genes in each pathway. The color of the bargraph indicates the significance of the enriched KEGG pathway,and the colorgradient represents the size of the p-value.

Figure 7

Diagram of molecular docking.(**A**)3D ligand interaction diagrams for docking poses of the gallic acid in the active site of TNF,IL-1β,TLR4,Alb, (**B**)3D ligan-d interaction diagrams for docking poses of the ellagic acid in the active site of TNF,IL-1β,TLR4,Alb, (**C**)3D ligand interaction diagrams for docking poses of the shikonin in the active site of TNF,IL-1β,TLR4,Alb,

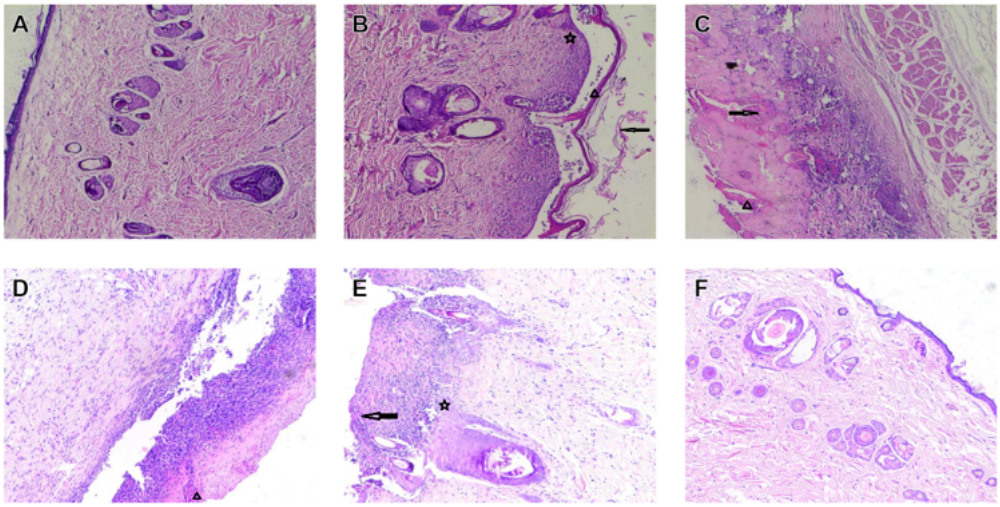

Triangle: hyperkeratosis, arrowhead: parakeratosis, pentagram: hypertrophy

Figure 8

Dermatological observation of rats in each group (HE, ×100).(**A**)Normal group, (**B**)model group, (**C**)Positive group, (**D**)CTGO low-dose Group, (**E**)CTGO middle-dose group, (**F**)CT-GO high-dose group,

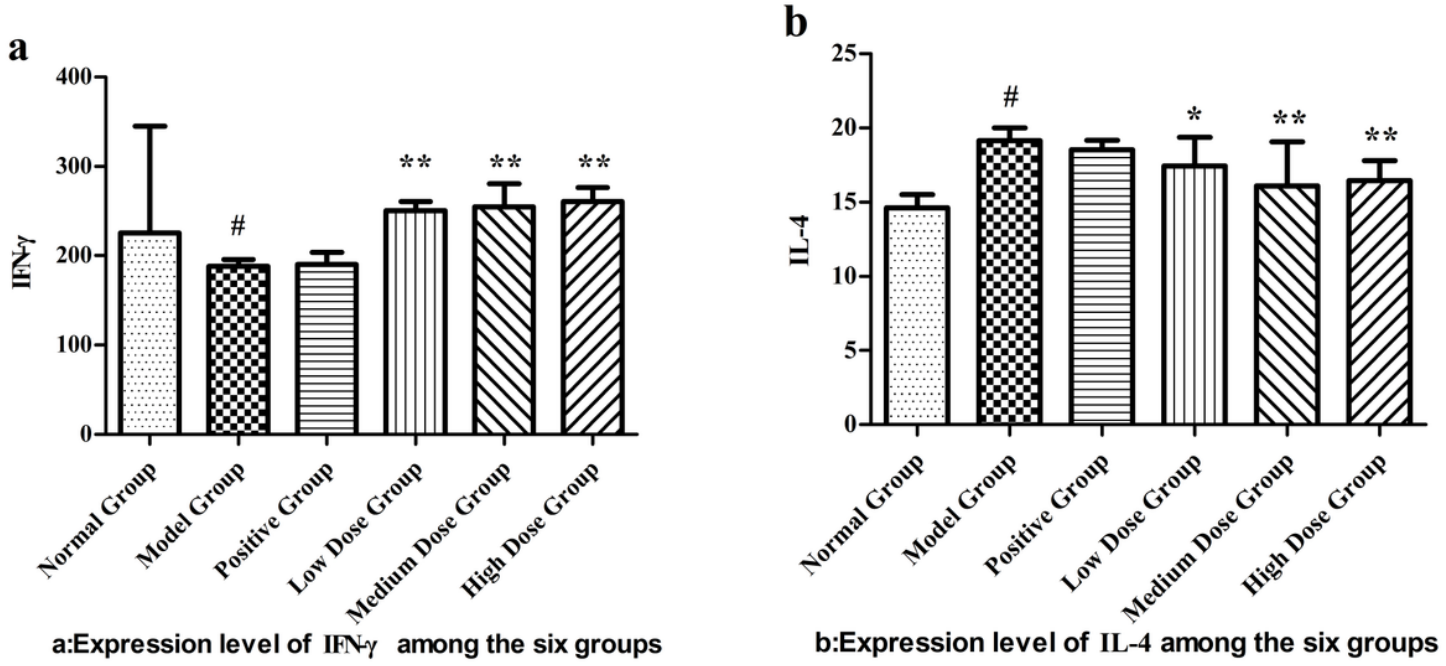

Figure 9

Detection of serum indexes in rats(x±s,n=10).Compared to the blank control group $^{\#}p < 0.05$, compared to the model control group $^{*}p < 0.05$, $^{**}p < 0.01$

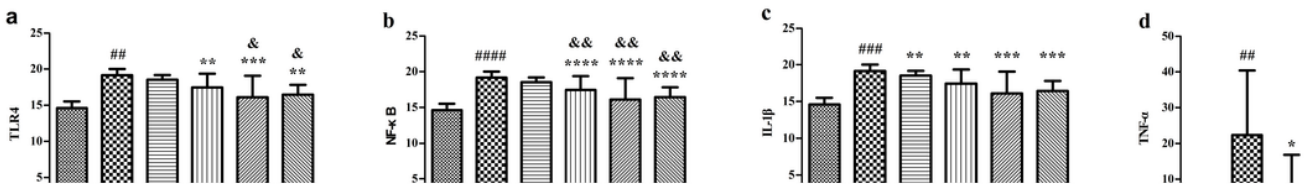

Figure 10

mRNA expression levels in skin tissue of each group of rats.Compared to the blank control group$^{\#\#}p < 0.01$,$^{\#\#\#}p < 0.001$,$^{\#\#\#\#}p < 0.0001$, compared to the model control group $^{*}p < 0.05$, $^{**}p < 0.01$, $^{***}p < 0.001$, $^{****}p < 0.0001$, compared to the positive group$^{\&}p < 0.05$, $^{\&\&}p < 0.01$